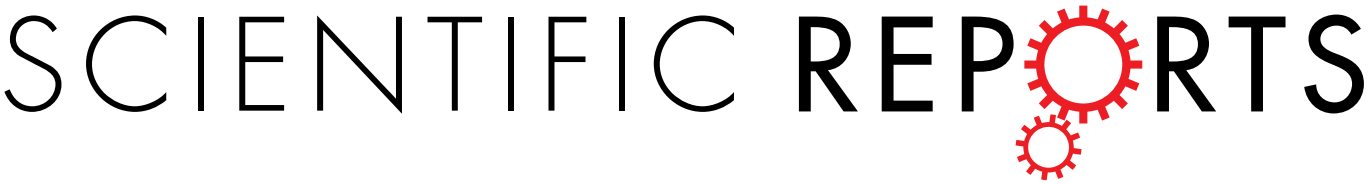

OPEN

Robust quantum switch with Rydberg excitations

Jing Qian[1,2]

Received: 19 July 2017
Accepted: 12 September 2017
Published online: 11 October 2017

We develop an approach to realize a quantum switch for Rydberg excitation in atoms with *Y- typed* level configuration. We find that the steady population on two different Rydberg states can be reversibly exchanged in a controllable way by properly tuning the Rydberg-Rydberg interaction. Moreover, our numerical simulations verify that the switching scheme is robust against spontaneous decay, environmental disturbance, as well as the duration of operation on the interaction, and also a high switching efficiency is quite attainable, which makes it have potential applications in quantum information processing and other Rydberg-based quantum technologies.

Switch is a device that is capable of switching some kind of signals (e.g. current, voltage, energy, heat *et.al.*) between different pathways. Classical switch plays a vital role in electronics and signal processing. Extending such a concept into the quantum regime where the role of pathways is played by quantum states leads to the production of various quantum switches, such as the switchable acoustic meta-materials[1], the current switch in quantum dots[2,3], the superconducting switch[4], the fiber-optical switch[5] and so on. In particular, for achieving an all-optical quantum switch, one promising way is coupling the atoms to a microscopic high-finesse cavity[6–9] which can strongly enhance the light-atom interactions[10]. Such a quantum optical switch has many promising applications, ranging from quantum information processing to quantum metrology[11–14].

Recently, Rydberg atoms have been manifested as an ideal candidate to study single-photon all-optical switches[15–17] and transistors[18–20], mainly due to the presence of interatomic interactions[21,22]. The ultra-strong interaction between two Rydberg states gives rise to blockade effect, bringing on a strong enhancement for the light-atom interactions[23–25]. Moreover, the blockade effect can provide an efficient mechanism for controlling the quantum states of the atomic system itself. A simplest scheme can be carried out, for example in a two-atom system, it prohibits the excitation of the second atom when the first one has already been excited to the Rydberg state. That is, it allows to control one atom's excitation or not via the status of the other[26–28], achieving a switchable excitation between two atomic states.

In the present work we propose a new scheme of quantum switch based on two Rydberg atoms of same *Y-typed* four-level configurations[29]. The special level configuration has two different Rydberg states: one is weakly coupled to the intermediated state and the other is strongly-coupled. This enables two different excitation pathways labeled as "OFF" and "ON" by us [see Fig. 1(c)], which can be efficiently switched via the control of intrastate interaction of the strongly-coupled Rydberg state. The interstate interaction between different Rydberg states, as main disturbance for the status switch, is greatly suppressed by employing the feature of nS Rydberg states that the strength of van der Waals (vdWs) interaction is not affected by Zeeman effect[30]. The robustness of the switching scheme is confirmed by its low sensitivity to the other parameters of the system, such as the intra-state interaction of the weakly-coupled state, the decay rate of the intermediate state, and the duration time of the switching process. We present a detailed discussion of a realistic experimental implementation of the switch with ^{87}Rb atoms and predict that the final switching efficiency will reach as high as 0.92.

Model Description

Our model consists of two identical Rydberg atoms in frozen-gas limit. As presented in Fig. 1(a), each atom has a *Y-typed* level structure that the ground state $|g\rangle$ is coupled to the middle state $|m\rangle$ via a laser field with Rabi frequency Ω_p and detuning Δ, and $|m\rangle$ is further resonantly coupled to two different Rydberg states $|s\rangle$ and $|r\rangle$ with Rabi frequencies ω and Ω, respectively. The Hamiltonian for a single atom k reads ($\hbar = 1$ everywhere)

[1]Department of Physics, School of Physics and Material Science, East China Normal University, Shanghai, 200062, People's Republic of China. [2]Collaborative Innovation Center of Extreme Optics, Shanxi University, Taiyuan, Shanxi, 030006, People's Republic of China. Correspondence and requests for materials should be addressed to J.Q. (email: jqian1982@gmail.com)

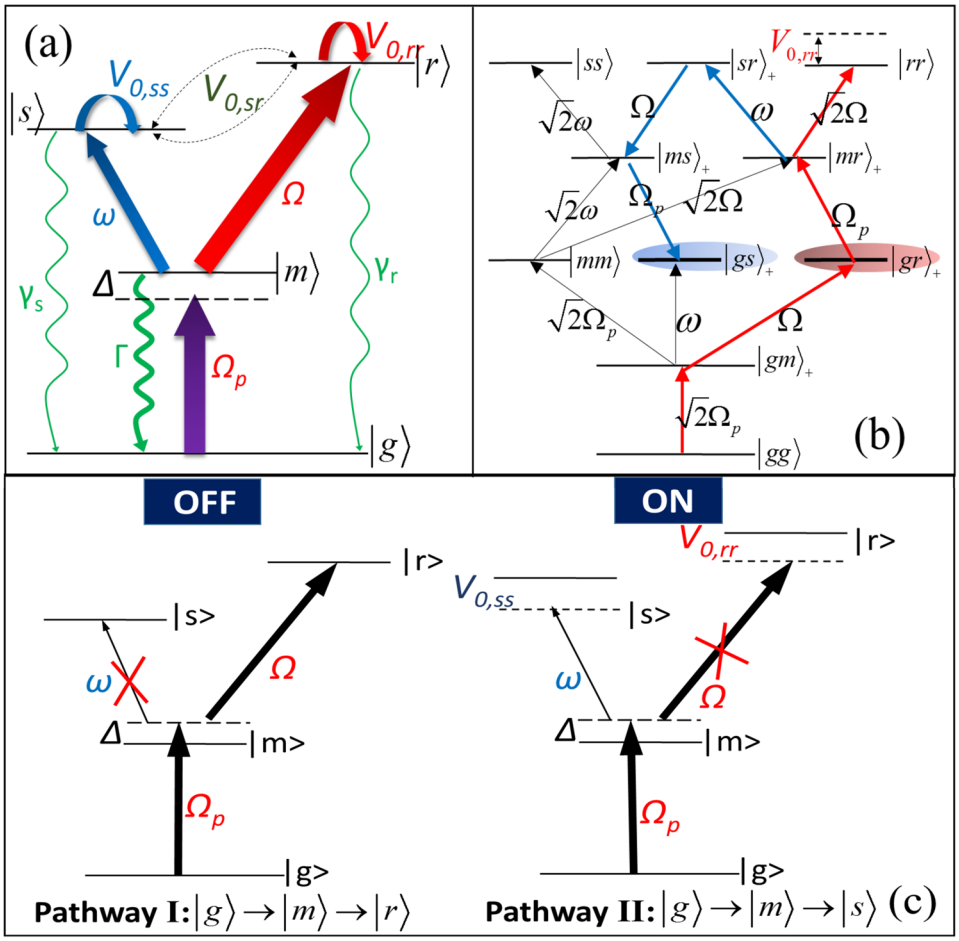

Figure 1. (**a**) Level structure of a single atom we adopted with the detailed descriptions about level couplings in the main text. (**b**) Level structure of two interacting atoms with the interstate transitions and the corresponding Rabi frequencies marked out. (**c**) Two possible pathways for exciting atoms into Rydberg states $|s\rangle$ and $|r\rangle$. For $\Omega > \omega$ and the interaction $\mathcal{V}_{0,rr} = 0$, the atom will be excited to the strongly-coupled state $|r\rangle$ through pathway I, defined as the "OFF" status of the switch; if $\mathcal{V}_{0,rr} \neq 0$ the atom prefers the excitation to the weakly-coupled state $|s\rangle$ through pathway II, defined as the "ON" status. For both cases the interaction strength $\mathcal{V}_{0,sr} = 0$ and $\mathcal{V}_{0,ss}$ is arbitrary.

$$\mathcal{H}_k = \Delta\sigma_{mm}^{(k)} + (\Omega_p\sigma_{gm}^{(k)} + \Omega\sigma_{mr}^{(k)} + \omega\sigma_{ms}^{(k)} + H.c.), \tag{1}$$

where the atomic operators $\sigma_{\alpha\beta}^{(k)} = |\alpha_k\rangle\langle\beta_k|, \alpha, \beta \in \{g, m, s, r\}$.

The properties of the interaction between atoms are dependent on the Rydberg states we chose. For nS Rydberg states, in the absence of electrostatic field the interaction is dominant by the second-order dipole-dipole interaction (i.e. vdWs interaction)[31]. It can be further classified as (i) the intrastate interaction $\mathcal{V}_{ss(rr)} = \mathcal{V}_{0,ss(rr)}|ss(rr)\rangle\langle ss(rr)|$ with the strength $\mathcal{V}_{0,ss(rr)} = C_6^{s(r)}/R^6$, which presents if both atoms settle in a same Rydberg state $|s\rangle$ or $|r\rangle$, (ii) the interstate interaction $\mathcal{V}_{sr} = \mathcal{V}_{0,sr}(|sr\rangle\langle rs| + |rs\rangle\langle sr|)$ for atoms in different Rydberg states with $\mathcal{V}_{0,sr} = C_6^{sr}/R^6$. Here R represents the separation between atoms, $C_6^{s,r,sr}$ are the interaction coefficients, and $|\alpha\beta\rangle \equiv |\alpha\rangle_1 \otimes |\beta\rangle_2$ are the two-atom states. Then the total Hamiltonian $\mathcal{H}$ is obtained from the sum of $\mathcal{H}_{k=1,2}$ and the interaction terms,

$$\mathcal{H} = \mathcal{H}_1 + \mathcal{H}_2 + \mathcal{V}_{ss} + \mathcal{V}_{rr} + \mathcal{V}_{sr}. \tag{2}$$

For a single atom, there exist two different pathways for excitation, I:$|g\rangle \rightarrow |m\rangle \rightarrow |r\rangle$ and II:$|g\rangle \rightarrow |m\rangle \rightarrow |s\rangle$. We consider the condition $\Omega > \omega$ so state $|r\rangle$ is the strongly-coupled state and the excitation pathway I is preferred, while $|s\rangle$ is the weakly-coupled state and the pathway II is less taken. Considering the long lifetime of states $|s\rangle$ and $|r\rangle$, their spontaneous decays γ_s and γ_r are far less than the decay Γ for state $|m\rangle$. For simplicity, we first assume $\Omega_p = \Omega$, $\Delta = 0$ and $\gamma_s = \gamma_r = \gamma$. As shown in Fig. 1(c), if $\Omega \gg \omega$, it is easy to envision that there is a steady state that almost 1/2 population transfers from $|g\rangle$ to $|r\rangle$ through pathway I with no population on $|m\rangle$ or $|s\rangle$, which is labeled as "OFF" state. However, we will show that considerable population would counter-intuitively

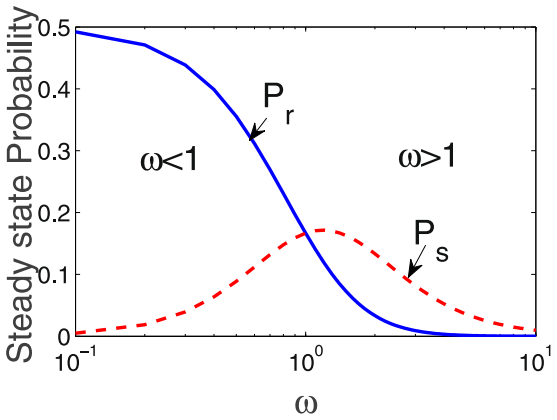

Figure 2. For the single-atom case, the steady probabilities of Rydberg state $|r\rangle$ (blue solid) and $|s\rangle$ (red dashed) are plotted as functions of ω (i.e. ω/Ω) with the decays $\gamma = 0.001$ and $\Gamma = 1.0$. Note that all frequency quantities are scaled by Ω.

transfer into the weakly-coupled state $|s\rangle$ through pathway II once the interaction $\mathcal{V}_{0,rr} \neq 0$. This process is found to be fully irrespective of the exact interaction strength $\mathcal{V}_{0,ss}$ and can serve as a controllable switch between the two status "OFF" and "ON" corresponding to different Rydberg excitations.

Single-atom case

We begin with the status "OFF" which can be analyzed in single-atom frame due to the absence of Rydberg interaction. The analytical expression for steady state can be obtained by solving the master equation $\dot{\rho}_k = -i[\mathcal{H}_k, \rho_k] + \mathcal{L}_k[\rho_k]$ $(k = 1, 2)$ with ρ_k and $\mathcal{H}_k$ the single-atom density matrix and Hamiltonian, respectively. Here the Lindblad superoperator $\mathcal{L}_k[\rho]$ is given by

$$\begin{aligned}\mathcal{L}_k[\rho] &= \Gamma\left(\sigma_{gm}^{(k)}\rho_k\sigma_{mg}^{(k)} - \frac{\{\sigma_{mm}^{(k)}, \rho_k\}}{2}\right) + \gamma\left(\sigma_{gs}^{(k)}\rho_k\sigma_{sg}^{(k)} - \frac{\{\sigma_{ss}^{(k)}, \rho_k\}}{2}\right) \\ &\quad + \gamma\left(\sigma_{gr}^{(k)}\rho_k\sigma_{rg}^{(k)} - \frac{\{\sigma_{rr}^{(k)}, \rho_k\}}{2}\right),\end{aligned} \tag{3}$$

which describes the effect of spontaneous decays from states $|m\rangle, |s\rangle$, and $|r\rangle$. In the following calculations, we use Ω (Ω^{-1}) as the frequency (time) unit, leading to normalized parameters as $\Omega_p \to \Omega_p/\Omega$, $\omega \to \omega/\Omega$, $\Gamma \to \Gamma/\Omega$, $\gamma \to \gamma/\Omega$, $\Delta \to \Delta/\Omega$, $\mathcal{V}_{0,rr(ss)} \to \mathcal{V}_{0,rr(ss)}/\Omega$, $\mathcal{V}_{0,sr} \to \mathcal{V}_{0,sr}/\Omega$, and $t \to \Omega t$. Then the steady populations of $|r\rangle$ and $|s\rangle$ are

$$P_r = \frac{1}{\frac{4\Gamma(1+\omega^2)+\gamma(8+\Gamma^2)}{16}\frac{4+\gamma(\Gamma+\gamma)}{\Gamma+\gamma} + \frac{(1+\omega^2)\Gamma\gamma+4(1+\omega^2)^2}{4}} \tag{4}$$

$$P_s = \omega^2 P_r \tag{5}$$

satisfying $P_s < P_r$ due to $\omega < 1$. In the limit $\omega \ll 1$ and due to $\Gamma \gg \gamma$, Eq. (4) reduces to $P_r \to 1/2$ and $P_s \to 0$, coinciding with our previous predictions about the status "OFF". In Fig. 2, we plot P_r and P_s as functions of ω, which shows that P_r decays and P_s grows up as ω increases and they become equal at $\omega = 1$. For further increased ω, both of them decrease but at different rates. The monotonous decrease of P_r is easy to understand, while the variation of P_s is ascribed to the electromagnetically induced transparency (EIT) effect in pathway II. A unique feature of the effect is that the excitation probability decreases as enhancing the coupling laser strength[32].

Two-atom Case

Turning to the picture of two interacting atoms, if the initial state is $|gg\rangle$, the total Hamiltonian $\mathcal{H}$ can be expanded by the ten symmetric two-atom bases only, $\{|gg\rangle, |mm\rangle, |ss\rangle, |rr\rangle, |gm\rangle_+, |gs\rangle_+, |gr\rangle_+, |ms\rangle_+, |mr\rangle_+, |sr\rangle_+\}$ where $|\alpha\beta\rangle_\pm = (|\alpha\beta\rangle \pm |\beta\alpha\rangle)/\sqrt{2}$, with the asymmetric states $|\alpha\beta\rangle_-$ safely ignored[33]. The coupling strategie and strength among them are presented in Fig. 1(b). In the absence of all Rydberg interaction, the population transfer is mainly following the approach $|gg\rangle \to |gm\rangle_+ \to |gr\rangle_+ \to |mr\rangle_+ \to |rr\rangle$ (red arrows) due to the stronger coupling strengths $(\propto\Omega)$. Finally, the long-lived states $|gg\rangle$, $|gr\rangle_+$ and $|rr\rangle$ are stably populated. Less population is found to accumulate in middle states $|gm\rangle_+$ and $|mr\rangle_+$ for their short lifetimes, and in $|mm\rangle$ and $|gs\rangle_+$ for their large decay rate Γ and small coupling strength ω, respectively. The steady populations are $P_{gr_+} \approx 0.5$ and $P_{gs_+} \approx 0$ which is same as the status "OFF" analyzed in the single-atom case. Note that $P_{gg} + P_{rr} = 1 - P_{gr_+} \approx 0.5$. Once

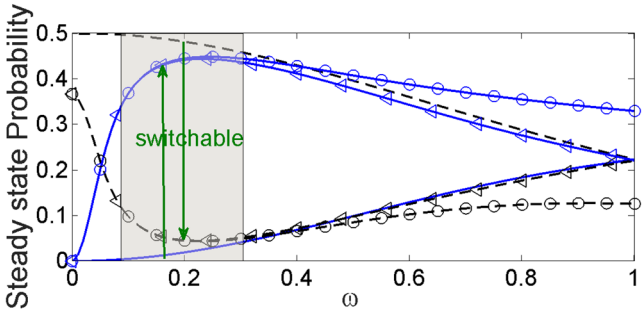

Figure 3. Steady probabilities P_{gs_+} (blue) and P_{gr_+} (black) as functions of ω (i.e. ω/Ω) with different intrastate interactions $\mathcal{V}_{0,rr}$ and $\mathcal{V}_{0,ss}$. The interstate interaction $\mathcal{V}_{0,sr}$ is kept at zero. The shaded area of $\omega \in (0.1,0.3)$ is suitable for switching. Relevant parameters are described in the main text.

the intrastate interaction $\mathcal{V}_{0,rr}$ is nonzero, giving rise to an energy shift on state $|rr\rangle$, the transition from $|mr\rangle_+$ to $|rr\rangle$ will be affected. If the condition for strong blockade, $\mathcal{V}_{0,rr} > \sqrt{2}$, is satisfied[24], the transition to the doubly Rydberg excited state will be fully suppressed. Instead, the population moves towards $|sr\rangle_+$ when the interstate interaction $\mathcal{V}_{0,sr} = 0$, which leads to the second transition pathway $|mr\rangle_+ \rightarrow |sr\rangle_+ \rightarrow |ms\rangle_+ \rightarrow |gs\rangle_+$ (blue arrows). Finally the steady populations are $P_{gr_+} \approx 0$ and $P_{gs_+} \approx 0.5$, corresponding to the status "ON" for our quantum switch. P_{sr_+} is also dominantly occupied besides P_{gs_+} and $P_{gg} \approx 0$.

The above qualitative analysis have been verified by numerically solving the master equation of two atoms, $\dot{\rho} = -i[\mathcal{H}, \rho] + \mathcal{L}_1[\rho] + \mathcal{L}_2[\rho]$, in which ρ is replaced by a two-atom density matrix. The steady populations P_{gr_+} and P_{gs_+} for states $|gr\rangle_+$ and $|gs\rangle_+$ are illustrated as functions of ω in Fig. 3 for three different cases: (i) $\mathcal{V}_{0,rr} = \mathcal{V}_{0,ss} = 0$ (the black dashed curve for P_{gr_+} and the blue solid curve for P_{gs_+}), (ii) $\mathcal{V}_{0,rr}$=1.0 and $\mathcal{V}_{0,ss} = 0$ (the black dashed curve with circles for P_{gr_+} and the blue solid curve with circles for P_{gs_+}), and (iii) $\mathcal{V}_{0,rr} = 1.0$ and $\mathcal{V}_{0,ss} = 1.0$ (the black dashed curve with triangles for P_{gr_+} and the blue solid curve with triangles for P_{gs_+}). In case (i) we find $P_{gr_+} \approx 0.5$ and $P_{gs_+} \approx 0.0$ at $\omega \ll 1$ and they two become equal as ω increases to 1, same as in Fig. 2 obtained in the single-atom frame. When the intrastate interaction $\mathcal{V}_{0,rr}$ is present, see the cases (ii) and (iii), there is a counterintuitive reversal of P_{gr_+} and P_{gs_+} at $\omega \geq 0.05$, indicating a large fraction of population transferred from $|gr\rangle_+$ to $|gs\rangle_+$. In the shadow region of $0.1 \leq \omega \leq 0.3$, P_{gs_+} and P_{gr_+} attain peak and off-peak values, respectively. Especially, by comparing cases (ii) and (iii) we find their variations are quite insensitive to the interaction strength $\mathcal{V}_{0,ss}$ in this region, which is ideally suited for operating this quantum switch.

The Switch Efficiency

To investigate the performance of the quantum switch, we first define the switching efficiency as

$$\eta = \frac{P_{gs_+}^{on}}{P_{gr_+}^{off}}, \tag{6}$$

where $P_{gr_+}^{off}$ and $P_{gs_+}^{on}$ are the steady population of $|gr\rangle_+$ in status "OFF" and of $|gs\rangle_+$ in status "ON", respectively. The status is switched by turning up or down the interaction $\mathcal{V}_{0,rr}$. For a ideal switch the population $P_{gs_+}^{on} = P_{gr_+}^{off} = 0.5$ and the efficiency $\eta = 1$.

In Fig. 4(a-c) we show the dependence of η on the interaction strength $\mathcal{V}_{0,rr}$ under the different relative couplings ω (ω is already normalized by Ω). For comparison, the steady populations P_{gs_+} (blue dashed) and P_{gr_+} (black dotted) are presented in the same frame. η reaches a saturation value and no longer changes with $\mathcal{V}_{0,rr}$ once $\mathcal{V}_{0,rr} > \sqrt{2}$, satisfying the two-atom strong blockade condition[24]. This brings us a big advantage at selections of state $|r\rangle$ in practice, especially for the atoms with multiple Rydberg energy levels. Besides, the saturation value of η is observed to be enhanced with the increase of ω, which is attributed to the slight changes of $P_{gr_+}^{off}$ (green dot) and $P_{gs_+}^{on}$ (blue dashed curve). For instance, in the case of $\omega = 0.3$ the saturated $\eta \rightarrow 0.978$. In the opposite case of $\mathcal{V}_{0,rr} < \sqrt{2}$, η and $P_{gs_+}^{on}$ rapidly falls to zero with the decrease of $\mathcal{V}_{0,rr}$.

Except for $\mathcal{V}_{0,rr}$ and ω, we also explore the influence of other parameters on the switching scheme, including the interaction $\mathcal{V}_{0,ss}$ of the weakly-coupled Rydberg state, the spontaneous decay Γ of the middle state, and the Rabi frequency Ω_p. In Fig. 5(a) we find that η keeps constant with $\mathcal{V}_{0,ss}$. This is due to the isolation of state $|ss\rangle$ from the transfer pathway as presented in Fig. 1(b), so that the energy shift of $|ss\rangle$ induced by interaction $\mathcal{V}_{0,ss}$ has no effect on η. However, an off-resonant transition $|g\rangle \rightarrow |m\rangle$ characterized by detuning Δ will reduce the steady population of Rydberg state, resulting in a decrease of η. We find that the switching scheme is robust to the middle-state decay Γ. As displayed in Fig. 5(b), η keeps almost unvaried in a broad regime of $1.0 < \Gamma < 10$ and start to slowly decrease only when $\Gamma > 10$. In contrast, a larger decay γ means a quick decay from Rydberg states, which directly causes a drop of η.

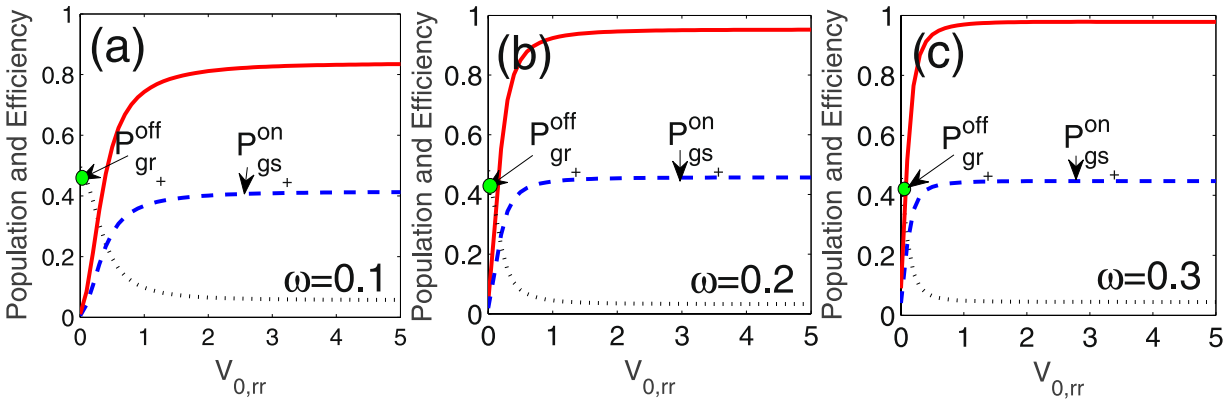

Figure 4. Steady populations P_{gr_+} (black dotted) and P_{gs_+} (blue dashed), and the switch efficiency η (red solid) versus the interaction strength $\mathcal{V}_{0,rr}$ in the cases of (**a**) $\omega = 0.1$, (**b**) $\omega = 0.2$ and (**c**) $\omega = 0.3$. ω is normalized by the Rabi frequency Ω. $P^{off}_{gr_+}$ is the value of P_{gr_+} at $\mathcal{V}_{0,rr} = 0$, marked by the green point, and $P^{on}_{gs_+}$ is same as P_{gs_+}.

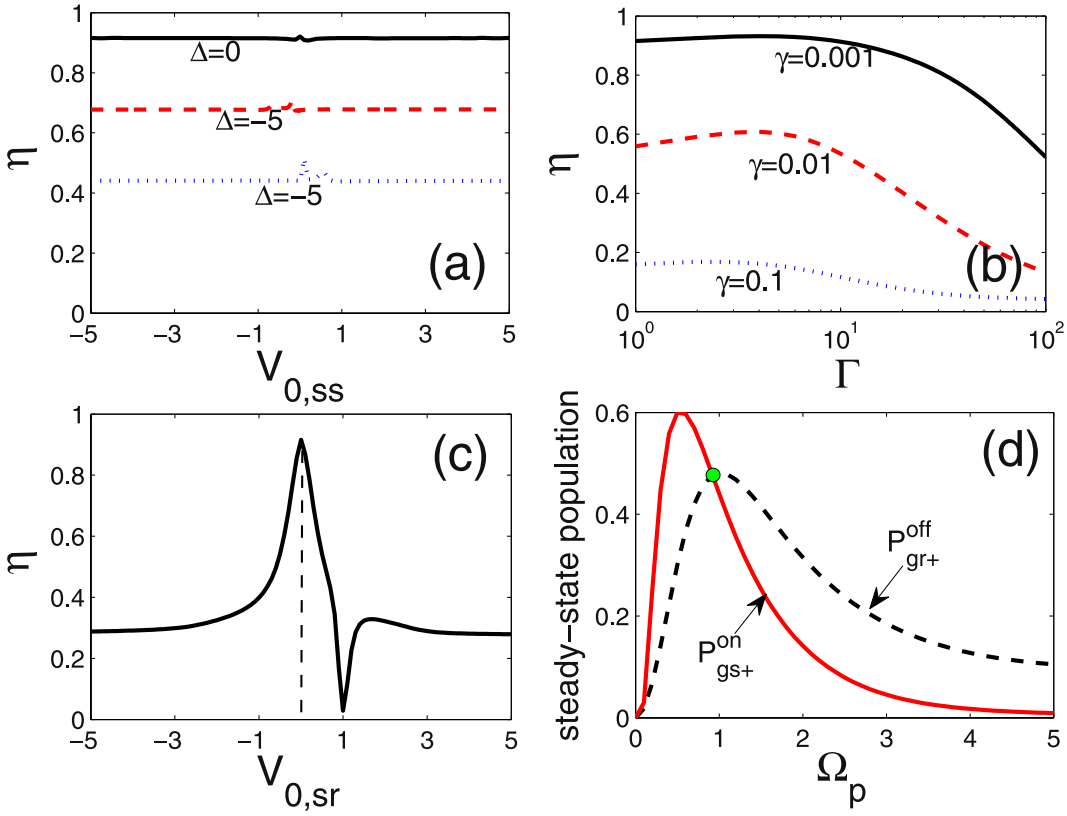

Figure 5. The switching efficiency η as a function of (**a**) the intrastate interaction $\mathcal{V}_{0,ss}$ for $\Delta = 0, -5, 5$ and the other parameters $\Gamma = 1.0, \gamma = 0.001, \mathcal{V}_{0,sr} = 0$; (**b**) the decay Γ from intermediate state for the Rydberg-state decay $\gamma = 0.001, 0.01, 0.1$ and the other parameters $\mathcal{V}_{0,ss} = 1.0, \mathcal{V}_{0,sr} = 0, \Delta = 0$; (**c**) the interstate exchange interaction $\mathcal{V}_{0,sr}$ for the other parameters $\mathcal{V}_{0,ss} = 1.0, \Gamma = 1.0, \gamma = 0.001, \Delta = 0$. Additionally, $\omega = 0.2$ and $\mathcal{V}_{0,rr} = 1.0$. The steady-state population P^{off}_{gr+} and P^{on}_{gs+} as a function of the driving laser Ω_p are shown in (**d**). All frequencies are scaled by Ω.

In addition to the parameters above, it should be stressed that the interstate interaction $\mathcal{V}_{0,sr}$ strongly destroys the switching efficiency. As shown in Fig. 5(c), η rapidly decreases as long as $|\mathcal{V}_{0,sr}| \neq 0$. That is because a nonzero $\mathcal{V}_{0,sr}$ will shift level $|sr\rangle_+$ and hinder the transition from $|mr\rangle_+$ to $|sr\rangle_+$, see Fig. 1(b). Worse, the competition between transitions of $|mr\rangle_+ \rightarrow |rr\rangle_+$ and $|mr\rangle_+ \rightarrow |sr\rangle_+$ is most serious when $\mathcal{V}_{0,sr} = \mathcal{V}_{0,rr}$, resulting in a near zero η. So the suppression of $\mathcal{V}_{0,sr}$ is a crucial condition for our approach of quantum switching. It can be guaranteed if we choose two nS states with large difference in principle quantum numbers n as Rydberg states. In the

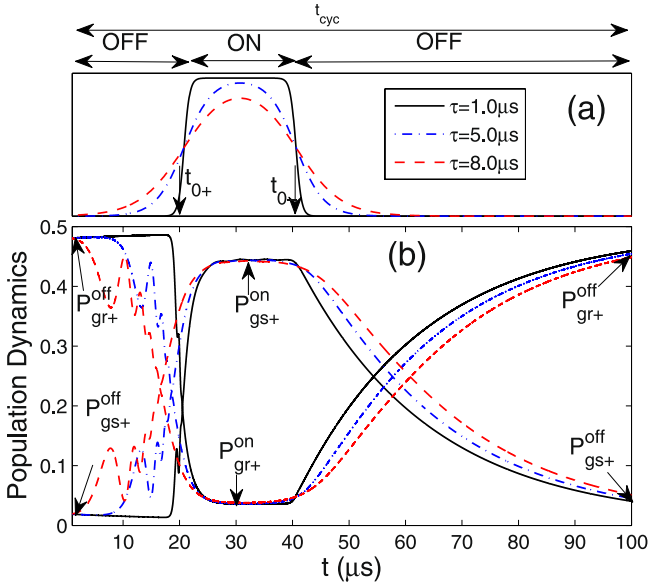

Figure 6. (**a**) Time dependence of interaction $V_{0,rr}(t)$ in the switching process for different optical switching durations $\tau = 1.0\,\mu$s (black solid), $5.0\,\mu$s (blue dash-dotted) and $8.0\,\mu$s (red dashed); (**b**) The dynamical evolution of the population $P_{gr_+}(t)$ and $P_{gs_+}(t)$ under the sequence of $V_{0,rr}(t)$ in a normal and reverse order. The parameters adopted in the simulation are described in the main text.

absence of applied electrostatic fields, the interstate interactions are negligible compared with the intrastate interactions, which has been confirmed theoretically[34,35] as well as experimentally[36].

Finally, we consider a more general case $\Omega_p \neq 1.0$ (i.e. $\Omega_p \neq \Omega$). Since the common limit $P^{on}_{gs_+} = P^{off}_{gr_+} = 0.5$ is unable to maintain in this case, the definition of η is no longer rigorous. We then show P^{off}_{gr+} and P^{on}_{gs+} versus Ω_p individually in Fig. 5(d). As the increase of Ω_p, P^{off}_{gr+} (black dashed) exhibits a clear reduction after reaching its maximum value 0.5 at $\Omega_p = 1.0$. Similar trends are observed in P^{on}_{gs+} (red solid) but the maximum 0.6 appears at about $\Omega_p \approx 0.6$. The reductions are because that for a large Ω_p the transition of $|gm\rangle_+ \rightarrow |mm\rangle$ is enhanced which results in a decrease of excitations to $|gs\rangle_+$ and $|gr\rangle_+$, see Fig. 1(b). Hence, we conclude that $\Omega_p = 1.0$ is an optimized value for our switching scheme, because the population of status "OFF" and "ON" are asymmetry for other values.

Experimental Implementation

After carefully researching the steady state of the switching system, we now turn to study the switching dynamics by numerically simulation with a series of experimental parameters. We assume two ^{87}Rb atoms are respectively confined in two independent optical dipole traps whose separation R can be adjusted from $15\,\mu$m to $4.0\,\mu$m by changing the incidence angle of the optical beams in a duration τ of the orders of several μs[24,37]. For the atomic states $|g\rangle = |5s_{1/2}\rangle, |m\rangle = |5p_{3/2}\rangle$, and Rydberg nS states $|s\rangle = |47s\rangle, |r\rangle = |65s\rangle$, the vdWs intrastate interaction coefficients are $C_6^r/2\pi = 50.4$ GHz μm^6 and $C_6^r/2\pi = 1.0$ GHz μm^6, and the spontaneous decay rates are $\Gamma/2\pi = 6.1$ MHz, $\gamma_s/2\pi = 7$ kHz, and $\gamma_r/2\pi = 3$ kHz (the effective lifetime is approximately $140\,\mu$s and $320\,\mu$s for $|47s\rangle$ and $|65s\rangle$, respectively, at $50\,\mu$K)[38]. In our switching operation, the initial separation is $R = 15\,\mu$m, leading to the interaction strength $\mathcal{V}^{off}_{0,rr}/2\pi = 0.004$ MHz and $\mathcal{V}^{off}_{0,ss}/2\pi = 8 \times 10^{-5}$ MHz. When R is reduced to $4.0\,\mu$m, the interactions are enhanced to $\mathcal{V}^{on}_{0,rr}/2\pi = 12.3$ MHz and $\mathcal{V}^{on}_{0,ss}/2\pi = 0.24$ MHz. For Rydberg states $|47s\rangle$ and $|65s\rangle$, we have $C_6^r \gg C_6^s \gg C_6^{sr}$ due to the large difference in principle quantum numbers of the two Rydberg states[39], so that the interstate interaction $\mathcal{V}_{0,sr}$ is largely suppressed and can be safely neglected. The Rabi frequencies, $\Omega/2\pi = 10$ MHz and $\omega/2\pi = 2$ MHz, are typical of current experiments.

To simulate the variation of the interaction under control, we introduce a time-dependent pulse sequence of $\mathcal{V}_{0,rr(ss)}(t)$ for a complete switching cycle consisting of three status: OFF, ON, and OFF,

$$\mathcal{V}_{0,rr(ss)}(t) = \frac{\mathcal{V}^{on}_{0,rr(ss)} - \mathcal{V}^{off}_{0,rr(ss)}}{4}\left[1 + \tanh\left(\frac{t - t_{0_+}}{\tau}\right)\right] \times \left[1 - \tanh\left(\frac{t - t_{0_-}}{\tau}\right)\right] \tag{7}$$

where $\mathcal{V}^{on}_{0,rr(ss)}$ and $\mathcal{V}^{off}_{0,rr(ss)}$ take the previously estimated values of interaction strength for status "ON" and "OFF", respectively, τ is the switching duration characterizing the changing speed of the interaction, and t_{0_+} and t_{0_-} are the critical switching moments of $\mathcal{V}^{off}_{0,rr} \rightarrow \mathcal{V}^{on}_{0,rr}$ and $\mathcal{V}^{on}_{0,rr} \rightarrow \mathcal{V}^{off}_{0,rr}$, respectively. As shown in Fig. 6(a), the larger the τ is, the slower and smoother the switching operation between $\mathcal{V}^{off}_{0,rr}$ and $\mathcal{V}^{on}_{0,rr}$ is. The total duration of the switching cycle is $100\,\mu s$ which is less than the lifetime of the Rydberg states. As discussed before, the excitation is

independent on the interaction $\mathcal{V}_{0,ss}(t)$, so for simplicity we assume it has a similar tendency of change with $\mathcal{V}_{0,rr}(t)$ here.

The dynamical evolution of the population $P_{gr_+}(t)$ and $P_{gs_+}(t)$, in response to the variation of interaction $\mathcal{V}_{0,rr(ss)}$, are obtained by numerically solving the master equation and displayed in Fig. 6(b). Initially prepared in the two-atom ground state $|gg\rangle$, the system tends to be a steady state with $P^{off}_{gr_+} \to 0.5$, $P^{off}_{gs_+} \to 0.0$ when the external laser fields are carried out, so a slight tendency of increase(decrease) for $P^{off}_{gr_+}\left(P^{off}_{gs_+}\right)$ is realized during the time of $0 < t < 20\ \mu$s in the case of $\tau = 1.0\ \mu$s (black solid line). Two conversions are clearly present at $t_{0_+} = 20\ \mu$s and $t_{0_-} = 40\ \mu$s. When $0 < t < t_{0_+}$ the status "OFF" with the situation $P^{off}_{gr_+} \gg P^{off}_{gs_+}$ is maintained. A fast exchange of the population occurs around t_{0_+} due to the switch $\mathcal{V}^{off}_{0,rr} \to \mathcal{V}^{on}_{0,rr}$, leading to the status "ON" with the reversed situation $P^{on}_{gs_+} \gg P^{on}_{gr_+}$ during the following period of time $t_{0_+} < t < t_{0_-}$. The second conversion takes place around t_{0_-} when the interaction $\mathcal{V}_{0,rr}(t)$ is tuned down again, but at this time a longer period is required for the retrieval of the population for status "OFF" due to the different transition pathways. The significant oscillation of population appears only at the period $0 < t < t_{0_+}$ with a larger duration τ. This is because in status "OFF" except $|gr_+\rangle$, $|gg\rangle$ and $|rr\rangle$ are also stably occupied, the resonant excitation between $|gg\rangle$ and $|gr_+\rangle$ will give rise to a Rabi-like oscillation if the duration of the switch is long enough. As an opposite example, in status "ON" only $|sr_+\rangle$ is dominantly occupied except for $|gs_+\rangle$, so the resonant excitation between them is not isolated but suffers from a strong decoherence. Hence, when $t > t_{0_+}$, even if τ is large there is no oscillation but a smooth redistribution of the population via decay process, which requests a longer time determined by the lifetime of Rydberg states.

Based on our numerical simulations with practical parameters, a realistic switching efficiency is estimated as $\eta = P^{on}_{gs+}/P^{off}_{gr+} \approx 0.92$ with the total operating time $t_{cyc} = 100\ \mu$s. We stress this optimal value is obtained by theoretical calculations with practical parameters however it excludes the influences from all the technical errors in a real experiment, e.g. the instrument precision, the stability of system and so on.

Applications and Conclusions

The quantum switch we present here based on the controllable strong interaction between two Rydberg atoms, but different from the single-photon transistor with Rydberg blockade[18], it enables an efficient and compact transition between two symmetric singly Rydberg excited states $|gr\rangle_+$ and $|gs\rangle_+$. With appropriate applications and developments, this will broaden exciting perspectives on quantum information processing with Rydberg atoms. For example, owing to its long lifetime and entanglement[40], the singly excited states can become an excellent carrier of quantum information. Then the reversible and swift switch of these states is a requisite operation for implementation of information transfer and quantum computation. Especially, the considerable separation ($\sim 10\mu m$) between two Rydberg atoms in our design allows local operations on one of them individually, served with our switching on two-atom states, various quantum logic gates are hopefully realizable[41–44]. Besides, the Rydberg atomic pair-state interferometer has been experimentally realized[45] recently. A high-precision quantum switch between different Rydberg excitations can enrich its measurement objects and develop the application of Rydberg atoms in quantum metrology. Finally, Rydberg dressing has been proposed to realize a number of interesting phases in ultra-cold gases, such as rotons and solitons[46,47]. An extension of our switch in a many-atom case will allow a more complex structure of Rydberg dressing, which makes it possible to simulate various and exotic spin-dependent phases by Rydberg atoms[48].

To conclude, our work presents a robust and experimentally feasible scheme of quantum switch, implemented in a system of two interacting Rydberg atoms. Each atom has a *Y-typed* level structure with two highly-excited Rydberg states. We show that which Rydberg state to be excited can be simply and effectively controlled by opening or closing the intrastate interaction of the strongly-coupled Rydberg state. After systematically investigating the steady state and the dynamics of the system in a numerical way, we verify the robustness of the scheme by presenting its insensitivity to the self-interaction of the weakly-coupled Rydberg state, the decay of intermediate state, and the duration time for switching. Our method is suitable for two Rydberg *nS* states in which the interstate exchange interaction between them can be totally suppressed by considering two *nS* states with large different principle quantum numbers. More possibilities for the implementation with other energy levels may work, e.g. by applying an external electrostatic field[49]. We show a numerical simulation of switch operation in ^{87}Rb atoms under realistic experimental conditions and find the switch efficiency approaching as high as 0.92. A many-atom case maybe treated as a good extension to the current scheme in the future, requiring more attentions to complex energy levels and transitions. We also plan to develop the applications of such particular switch in the fields of quantum information processing and other quantum devices.

References

1. Wang, P., Casadei, F., Shan, S., Weaver, J. & Bertoldi, K. Harnessing buckling to design tunable locally resonant acoustic metamaterials. *Physical Review Letters* **113**, 014301 (2014).
2. Brandes, T. & Renzoni, F. Current switch by coherent trapping of electrons in quantum dots. *Physical Review Letters* **85**, 4148–4151 (2000).
3. Dessotti, F. *et al*. Unveiling majorana quasiparticles by a quantum phase transition: Proposal of a current switch. *Physical Review B* **94**, 125426 (2016).
4. Pechal, M. *et al*. Superconducting switch for fast on-chip routing of quantum microwave fields. *Physical Review Applied* **6**, 024009 (2016).
5. Shea, D., Junge, C., Volz, J. & Rauschenbeutel, A. Fiber-optical switch controlled by a single atom. *Physical Review Letters* **111**, 193601 (2013).
6. Davidovich, L., Maali, A., Brune, M., Raimond, J. & Haroche, S. Quantum switches and nonlocal microwave fields. *Physical Review Letters* **71**, 2360–2363 (1993).

7. Feng, X., Kwek, L., Lai, C. & Oh, C. Quantum computation based on a quantum switch in cavity qed. *Laser Physics* **16**, 1508–1511 (2006).
8. Chen, W. *et al*. All-optical switch and transistor gated by one stored photon. *Science* **341**, 768–770 (2013).
9. Tiecke, T. *et al*. Nanophotonic quantum phase switch with a single atom. *Nature* **508**, 241–244 (2014).
10. Haroche, S. & Raimond, J. Exploring the quantum: Atoms, cavities, and photons. *Oxford Univ. Press* (2006).
11. Briegel, H., Dür, W., Cirac, J. & Zoller, P. Quantum repeaters: The role of imperfect local operations in quantum communication. *Physical Review Letters* **81**, 5932–5935 (1998).
12. Escartín, J. & Posada, P. Delayed commutation in quantum computer networks. *Physical Review Letters* **97**, 110502 (2006).
13. Schirmer, S. & Ross, P. Fast high-fidelity information transmission through spin-chain quantum wires. *Physical Review A* **80**, 030301(R) (2009).
14. Qin, W. & Nori, F. Controllable single-photon transport between remote coupled-cavity arrays. *Physical Review A* **93**, 032337 (2016).
15. Escartín, J. & Posada, P. Counterfactual rydberg gate for photons. *Physical Review A* **85**, 032309 (2012).
16. Baur, S., Tiarks, D., Rempe, G. & Dürr, S. Single-photon switch based on rydberg blockade. *Physical Review Letters* **112**, 073901 (2014).
17. Li, W. & Lesanovsky, I. Coherence in a cold-atom photon switch. *Physical Review A* **92**, 043828 (2015).
18. Gorniaczyk, H., Tresp, C., Schmidt, J., Fedder, H. & Hofferberth, S. Single-photon transistor mediated by interstate rydberg interactions. *Physical Review Letters* **113**, 053601 (2014).
19. Tiarks, D., Baur, S., Schneider, K., Dürr, S. & Rempe, R. Single-photon transistor using a förster resonance. *Physical Review Letters* **113**, 053602 (2014).
20. Gorniaczyk, H. *et al*. Enhancement of rydberg-mediated single-photon nonlinearities by electrically tuned förster resonances. *Nat. Comm.* **7**, 12480 (2016).
21. Gallagher, T. & Pillet, P. Dipole-dipole interactions of rydberg atoms. *Adv. At. Mol. Opt. Phys.* **56**, 161–218 (2008).
22. Marcassa, L. & Shaffer, J. Interactions in ultracold rydberg gases. *Adv. At. Mol. Opt. Phys.* **63**, 47–133 (2014).
23. Heidemann, R. *et al*. Evidence for coherent collective rydberg excitation in the strong blockade regime. *Physical Review Letters* **99**, 163601 (2007).
24. Gaëtan, A. *et al*. Observation of collective excitation of two individual atoms in the rydberg blockade regime. *Nat. Phys.* **5**, 115–118 (2009).
25. Pritchard, J. *et al*. Cooperative atom-light interaction in a blockaded rydberg ensemble. *Physical Review Letters* **105**, 193603 (2010).
26. Jaksch, D. *et al*. Fast quantum gates for neutral atoms. *Physical Review Letters* **85**, 2208–2211 (2000).
27. Lukin, M. *et al*. Dipole blockade and quantum information processing in mesoscopic atomic ensembles. *Physical Review Letters* **87**, 037901 (2001).
28. Comparat, D. & Pillet, P. Dipole blockade in a cold rydberg atomic sample. *Journal of the Optical Society of America B* **27**, A208–A232 (2010).
29. Liu, Y. *et al*. Nonlinear modifications of photon correlations via controlled single and double rydberg blockade. *Physical Review A* **91**, 043802 (2015).
30. Walker, T. & Saffman, M. Consequences of zeeman degeneracy for the van der waals blockade between rydberg atoms. *Physical Review A* **77**, 032723 (2008).
31. Saffman, M., Walker, T. & Mø lmer, K. Quantum information with rydberg atoms. *Rev. Mod. Phys.* **82**, 2313–2363 (2010).
32. Gärttner, M., Whitlock, S., Schönleber, D. & Evers, J. Collective excitation of rydberg-atom ensembles beyond the superatom model. *Physical Review Letters* **113**, 233002 (2014).
33. Mø ller, D., Madsen, L. & Mø lmer, K. Quantum gates and multiparticle entanglement by rydberg excitation blockade and adiabatic passage. *Physical Review Letters* **100**, 170504 (2008).
34. Olmos, B., Li, W., Hofferberth, S. & Leasanovsky, I. Amplifying single impurities immersed in a gas of ultracold atoms. *Physical Review A* **84**, 041607 (2011).
35. Cano, D. & Fortágh, J. Multiatom entanglement in cold rydberg mixtures. *Physical Review A* **89**, 043413 (2014).
36. Teixeira, R., Avigliano, C., Nguyen, T., Moltrecht, T. & Raimond, J. Microwaves probe dipole blockade and van der waals forces in a cold rydberg gas. *Physical Review Letters* **115**, 013001 (2015).
37. Béguin, L., Vernier, A., Chicireanu, R., Lahaye, T. & Browaeys, A. Direct measurement of the van der waals interaction between two rydberg atoms. *Physical Review Letters* **110**, 263201 (2013).
38. Beterov, I., Ryabtsev, I., Ryabtsev, D. & Ryabtsev, V. Quasiclassical calculations of blackbody-radiation-induced depopulation rates and effective lifetimes of rydberg ns, np, and nd alkali-metal atoms with $n \leq 80$. *Physical Review A* **79**, 052504 (2009).
39. Levi, E., Miná, J., Garrahan, J. & Lesanovsky, I. Crystalline structures and frustration in a two-component rydberg gas. *New journal of Physics* **17**, 123017 (2015).
40. Johnson, J. & Rolston, S. Interactions between rydberg-dressed atoms. *Physical Review A* **82**, 033412 (2010).
41. Xia, T., Zhang, X. & Saffman, M. Analysis of a controlled phase gate using circular rydberg states. *Physical Review A* **88**, 062337 (2013).
42. Maller, K. *et al*. Rydberg-blockade controlled-not gate and entanglement in a two-dimensional array of neutral-atom qubits. *Physical Review A* **92**, 022336 (2015).
43. Beterov, I. *et al*. Two-qubit gates using adiabatic passage of the stark-tuned förster resonances in rydberg atoms. *Physical Review A* **94**, 062307 (2016).
44. Theis, L., Motzoi, F., Wilhelm, F. & Saffman, M. High-fidelity rydberg-blockade entangling gate using shaped, analytic pulses. *Physical Review A* **94**, 032306 (2016).
45. Nipper, J. *et al*. Atomic pair-state interferometer: Controlling and measuring an interaction-induced phase shift in rydberg-atom pairs. *Physical Review X* **2**, 031011 (2012).
46. Henkel, N., Nath, R. & Pohl, T. Three-dimensional roton excitations and supersolid formation in rydberg-excited bose-einstein condensates. *Physical Review Letters* **104**, 195302 (2010).
47. Pupillo, G., Micheli, A., Boninsegni, M., Lesanovsky, I. & Zoller, P. Strongly correlated gases of rydberg-dressed atoms: Quantum and classical dynamics. *Physical Review Letters* **104**, 223002 (2010).
48. Weimer, H., Müller, M., Lesanovsky, I., Zoller, P. & Büchler, H. A rydberg quantum simulator. *Nat. Phys.* **6**, 382–388 (2010).
49. Petrosyan, D. & Mø lmer, K. Binding potentials and interaction gates between microwave-dressed rydberg atoms. *Physical Review Letters* **113**, 123003 (2014).

Acknowledgements

J. Qian thanks J.F. Chen for providing useful timescales (a few microseconds) of adjusting the inter-atomic separation R in experiment. This work is supported by the NSFC under Grants No. 11474094, No. 11104076, the Specialized Research Fund for the Doctoral Program of Higher Education No. 20110076120004.

Additional Information

Competing Interests: The authors declare that they have no competing interests.

Publisher's note: Springer Nature remains neutral with regard to jurisdictional claims in published maps and institutional affiliations.